

Investigating the effect of U_1 vector leptoquark on $b \rightarrow u\tau\bar{\nu}$ mediated B decays

Suman Kumbhakar^{1,*} and Rukmani Mohanta^{2,†}

¹*Department of Physics, Indian Institute of Technology Bombay, Mumbai-400076, India*

²*School of Physics, University of Hyderabad, Hyderabad-500046, India*

Abstract

The recent measurements of lepton flavor universality (LFU) violating observables in semileptonic $b \rightarrow c\ell\bar{\nu}$ and $b \rightarrow s\ell^+\ell^-$ transitions by various experiments exhibit $(2 - 3)\sigma$ deviations from their corresponding Standard Model (SM) predictions. These tantalizing signals hint towards the possible role of new physics (NP) in $b \rightarrow c\tau\bar{\nu}$ and $b \rightarrow s\mu^+\mu^-$ decay channels. This in turn indicates that the same class of NP as appeared in $b \rightarrow c\tau\bar{\nu}$, might also show up in other tree level processes involving $b \rightarrow u\tau\bar{\nu}$ transition. Since these charged current transitions are doubly Cabibbo suppressed, the NP contributions could be significant enough leading to sizeable effects in some of the observables. In this paper, we study the implications of the vector leptoquark $U_1(3, 1, 2/3)$, which is one of the few scenarios that can simultaneously explain the LFU violation signals both in the charged-current as well as neutral-current sectors, on the semileptonic decays $B \rightarrow (\pi, \rho, \omega)\tau\bar{\nu}$ and $B_s \rightarrow (K, K^*)\tau\bar{\nu}$. In particular, we pay our attention to the branching fraction, lepton flavor non-universality (LNU) observable, forward-backward asymmetry and the polarization asymmetry parameters of these modes. We find substantial deviations in the branching fractions as well as LNU observables of these decay modes due to the U_1 contributions, which can be probed by the currently running experiments LHCb and Belle-II.

*Electronic address: suman@phy.iitb.ac.in

†Electronic address: rmsp@uohyd.ac.in

I. INTRODUCTION

The SM is a highly successful and well established theory beyond doubt and can explain almost all the observed data from the colliders. Though the LHC Run-II has ushered in a new era in terms of energy, luminosity and discovery potential, so far there is no unambiguous signal of NP beyond the Standard Model (BSM). On the other hand, several intriguing hints of discrepancies between the observed data and the SM predictions have been reported by the B -physics experiments, i.e., Belle, BaBar and LHCb, in the last few years. These discrepancies are mainly in the form of lepton flavor universality violations in semileptonic B decays associated with the charged current (CC) $b \rightarrow c\ell\bar{\nu}$ [1–9] and neutral current (NC) $b \rightarrow s\ell^+\ell^-$ [10–20] transitions. In the absence of any much anticipated direct NP signal at the LHC experiment, these tantalizing hints of LFU violating observables play a crucial role in exploring the BSM physics and thus have attracted immense attention in the last few years.

Sizeable deviations have been observed by three different experiments in the LFU observables of the charged-current channels, which are characterized as the ratios of branching fractions

$$R_{D^{(*)}} \equiv \frac{\text{Br}(B \rightarrow D^{(*)}\tau\bar{\nu})}{\text{Br}(B \rightarrow D^{(*)}\ell\bar{\nu})}, \quad (1)$$

with $\ell = e$ or μ and

$$R_{J/\psi} \equiv \frac{\text{Br}(B_c \rightarrow J/\psi\tau\bar{\nu})}{\text{Br}(B_c \rightarrow J/\psi\mu\bar{\nu})}. \quad (2)$$

These observables are considered as the clean probes of NP as the hadronic uncertainties inherent in individual branching fraction predictions canceled out to a large extent. The present world averages of $R_{D^{(*)}}$ measurements, performed by the Heavy Flavor Averaging Group (HFLAV) [21]

$$R_D^{\text{exp}} = 0.340 \pm 0.027 \pm 0.013, \quad R_{D^*}^{\text{exp}} = 0.295 \pm 0.011 \pm 0.008, \quad (3)$$

have 3.1σ deviations (including their correlation of -0.38) from the corresponding SM predictions $R_D^{\text{SM}} = 0.299 \pm 0.003$ (1.4σ) and $R_{D^*}^{\text{SM}} = 0.258 \pm 0.005$ (2.5σ) [21]. In the same line, the measured ratio $R_{J/\psi} = 0.71 \pm 0.17 \pm 0.18$ [22] also has 1.7σ deviation from its SM prediction, $R_{J/\psi}^{\text{SM}} = 0.289 \pm 0.010$ [23]. Moreover, the recent measurement of the longitudinal polarization of D^* meson in $B^0 \rightarrow D^{*-}\tau^+\bar{\nu}$ by Belle collaboration, $F_L^{D^*} = 0.60 \pm 0.08 \pm 0.04$ [24], also

differs from its SM value 0.46 ± 0.04 [25] by 1.6σ . These deviations primarily hint towards the possible interplay of NP in $b \rightarrow c\tau\bar{\nu}$ decay channels. Recently, these anomalies have been studied in various model independent techniques [26–36].

The LFU violation observables in the neutral current sector are associated with $b \rightarrow s\ell^+\ell^-$ transition and are described as

$$R_{K^{(*)}} \equiv \frac{\text{Br}(B \rightarrow K^{(*)}\mu^+\mu^-)}{\text{Br}(B \rightarrow K^{(*)}e^+e^-)}, \quad (4)$$

which also show around $(2 - 2.5)\sigma$ deviation from their SM values [16–20]. In addition, the measured values of the branching fraction of $B_s \rightarrow \phi\mu^+\mu^-$ [10, 13] and the angular observable P'_5 in $B \rightarrow K^*\mu^+\mu^-$ decay [11, 14, 15] differ from their SM predictions at the level of $(3 - 3.5)\sigma$. Assuming NP contributes only in $b \rightarrow s\mu^+\mu^-$ transition, it has been shown that the allowed NP solutions can be described in the form of vector and axial-vector operators. Recent global fit studies for this sector can be found in Refs. [37–42].

These observed hints of LFU violation have triggered a large number of detailed phenomenological studies trying to ascertain the nature of plausible NP explanation. As the $b \rightarrow c\ell\bar{\nu}$ CC transitions occur at the tree-level, while the NC transitions $b \rightarrow s\ell^+\ell^-$ appear one-loop level, the anomalies associated with these transitions probe essentially different NP scales. Therefore, most of the theoretical studies in the literature have attempted to address either NC or CC oddities, but not both on the same footing. There exists only few scenarios which can simultaneously accommodate both these anomalies and Leptoquark (LQ) model is one such possible framework [43–50]. The existence of LQs at low energy is predicted in many extensions of the standard model such as Grand unified theory (GUT) [51–54], Pati-Salam model [55–57], technicolor [58–60], composite model [61] etc.

Concerning the recent flavor anomalies, the U_1 vector LQ which transforms as $(3, 1, 2/3)$ under the SM gauge group $SU(3)_C \times SU(2)_L \times U(1)_Y$ is known to successfully elucidate them. Therefore, in this work, we would like to investigate in detail the effect of $U_1(3, 1, 2/3)$ LQ on another class of semileptonic rare B decays, mediated through $b \rightarrow u\tau\bar{\nu}$ transitions. We would like to emphasize here that, for $b \rightarrow c$ anomalies, it is customarily assumed that the NP is coupled only to the third generation leptons rather than the first two generations, i.e., in the $b \rightarrow c\tau\bar{\nu}$ processes. Hence, it is natural to expect that the same class of NP might also show up in the rare processes involving $b \rightarrow u\tau\bar{\nu}$ transition. Furthermore, as these CC transitions are doubly Cabibbo suppressed, the NP contributions could be significant

enough leading to sizeable effects in some of the observables. Recently, some groups have addressed different NP effects on various decays mediated by $b \rightarrow u$ transition [62–65].

The outline of the paper is as follows. In Section II, we discuss briefly the relevant effective Hamiltonian describing the semileptonic transitions $b \rightarrow (c, u)\ell\bar{\nu}$ and $b \rightarrow sl^+\ell^-$. The NP contributions arising from the exchange of vector LQ U_1 is presented in Section III. Section IV contains the discussion about our numerical fit technique and the constraints obtained on the NP parameters. The implications of vector LQ on various decay observables of $b \rightarrow u\tau\bar{\nu}$ processes are presented in section V and our conclusions are summarized in Section VI.

II. EFFECTIVE HAMILTONIANS FOR $b \rightarrow c(u)\tau\bar{\nu}$ AND $b \rightarrow sl^+\ell^-$

The most general effective Hamiltonian for the charged current transition $b \rightarrow c\tau\bar{\nu}$ can be written as

$$\mathcal{H}_{\text{eff}}^{b \rightarrow c} = \frac{4G_F}{\sqrt{2}} V_{cb} [(1 + C_{V_L}^{b \rightarrow c})\mathcal{O}_{V_L} + C_{V_R}^{b \rightarrow c}\mathcal{O}_{V_R} + C_{S_L}^{b \rightarrow c}\mathcal{O}_{S_L} + C_{S_R}^{b \rightarrow c}\mathcal{O}_{S_R} + C_T^{b \rightarrow c}\mathcal{O}_T], \quad (5)$$

where G_F is the Fermi constant and $V_{cb} = (42.2 \pm 0.08) \times 10^{-3}$ [66] is the Cabibbo-Kobayashi-Maskawa (CKM) matrix element. Here we assume that the neutrino is left-chiral. The operator \mathcal{O}_{V_L} is the SM four-fermion interaction which has the usual $(V - A) \times (V - A)$ structure, whereas $\mathcal{O}_{V_R, S_L, S_R, T}$ are the new operators which arise only in beyond the SM scenarios. The $C_i^{b \rightarrow c}$ ($i = V_L, V_R, S_L, S_R, T$) are the corresponding NP Wilson coefficients (WCs). The explicit forms of the SM as well as NP operators are

$$\begin{aligned} \mathcal{O}_{V_L} &= (\bar{c}\gamma_\mu P_L b)(\bar{\tau}\gamma^\mu P_L \nu), & \mathcal{O}_{V_R} &= (\bar{c}\gamma_\mu P_R b)(\bar{\tau}\gamma^\mu P_L \nu) \\ \mathcal{O}_{S_L} &= (\bar{c}P_L b)(\bar{\tau}P_L \nu), & \mathcal{O}_{S_R} &= (\bar{c}P_R b)(\bar{\tau}P_L \nu), & \mathcal{O}_T &= (\bar{c}\sigma_{\mu\nu} P_L b)(\bar{\tau}\sigma^{\mu\nu} P_L \nu), \end{aligned} \quad (6)$$

where $P_{L,R} = (1 \mp \gamma_5)/2$ are the chiral projection operators.

Analogously, the effective Hamiltonian for $b \rightarrow u\tau\bar{\nu}$ transition can be expressed as

$$\mathcal{H}_{\text{eff}}^{b \rightarrow u} = \frac{4G_F}{\sqrt{2}} V_{ub} [(1 + C_{V_L}^{b \rightarrow u})\mathbb{O}_{V_L} + C_{V_R}^{b \rightarrow u}\mathbb{O}_{V_R} + C_{S_L}^{b \rightarrow u}\mathbb{O}_{S_L} + C_{S_R}^{b \rightarrow u}\mathbb{O}_{S_R} + C_T^{b \rightarrow u}\mathbb{O}_T], \quad (7)$$

where $V_{ub} = (3.94 \pm 0.36) \times 10^{-3}$ [66] is the relevant CKM matrix element. The five operators \mathbb{O}_i for this transition take the same structure as in Eq. (6) with c quark being replaced by an u quark. The $C_i^{b \rightarrow u}$ are the NP WCs for $b \rightarrow u\tau\bar{\nu}$ transition.

The SM effective Hamiltonian for the FCNC decays mediated by the quark level transition $b \rightarrow s\ell^+\ell^-$ is

$$\mathcal{H}_{\text{SM}} = \frac{4G_F}{\sqrt{2}\pi} V_{tb} V_{ts}^* \left[\sum_{i=1}^6 C_i(\mu) \mathcal{O}_i(\mu) + C_7 \frac{e}{16\pi^2} [\bar{s}\sigma_{\mu\nu}(m_s P_L + m_b P_R)b] F^{\mu\nu} + C_9 \frac{\alpha_{em}}{4\pi} (\bar{s}\gamma^\mu P_L b)(\bar{\ell}\gamma_\mu \ell) + C_{10} \frac{\alpha_{em}}{4\pi} (\bar{s}\gamma^\mu P_L b)(\bar{\ell}\gamma_\mu \gamma_5 \ell) \right],$$

where V_{tb} and V_{ts} are the CKM matrix elements and α_{em} is the fine structure constant. The effect of the operators \mathcal{O}_i , $i = 1 - 6, 8$ can be embedded in the redefined effective WCs as $C_7(\mu) \rightarrow C_7^{\text{eff}}(\mu, q^2)$ and $C_9(\mu) \rightarrow C_9^{\text{eff}}(\mu, q^2)$.

We consider the addition of vector and axial-vector NP operators to the SM effective Hamiltonian of $b \rightarrow s\mu^+\mu^-$. Consequently, the effective Hamiltonian takes the form

$$\mathcal{H}_{\text{eff}}^{b \rightarrow s} = \mathcal{H}_{\text{SM}} + \mathcal{H}_{\text{VA}}, \quad (8)$$

where \mathcal{H}_{VA} is expressed as

$$\mathcal{H}_{\text{VA}} = \frac{\alpha_{em} G_F}{\sqrt{2}\pi} V_{tb} V_{ts}^* \left[C_9^{\text{NP}} (\bar{s}\gamma^\mu P_L b)(\bar{\mu}\gamma_\mu \mu) + C_{10}^{\text{NP}} (\bar{s}\gamma^\mu P_L b)(\bar{\mu}\gamma_\mu \gamma_5 \mu) + C_9^{\prime\text{NP}} (\bar{s}\gamma^\mu P_R b)(\bar{\mu}\gamma_\mu \mu) + C_{10}^{\prime\text{NP}} (\bar{s}\gamma^\mu P_R b)(\bar{\mu}\gamma_\mu \gamma_5 \mu) \right]. \quad (9)$$

Here $C_{9,10}^{\text{NP}}$ and $C_{9,10}^{\prime\text{NP}}$ are the NP WCs. Considering one operator at a time, it has been shown in Ref. [37], that there are only three possible NP solutions: (I) $C_9^{\text{NP}} = -1.09 \pm 0.18$, (II) $C_9^{\text{NP}} = -C_{10}^{\text{NP}} = -0.53 \pm 0.09$ and (III) $C_9^{\text{NP}} = -C_{10}^{\text{NP}} = -1.12 \pm 0.17$, which can account for present data in this sector.

III. NP EFFECTS IN VECTOR LQ MODEL

We now consider the effect of vector LQ $U_1(3, 1, 2/3)$ on these decay processes. This LQ can explain the anomalies in both $b \rightarrow c\tau\bar{\nu}$ and $b \rightarrow s\mu^+\mu^-$ transitions [49, 50]. The interaction Lagrangian of U_1 LQ with the SM fermions can be written as

$$\mathcal{L}_{\text{LQ}}^{U_1} = h_L^{ij} \bar{Q}_{iL} \gamma_\mu L_{jL} U_1^\mu + h_R^{ij} \bar{d}_{iR} \gamma_\mu l_{jR} U_1^\mu + h.c., \quad (10)$$

where $h_{L,R}^{ij}$ are the couplings of U_1 to quark and lepton pairs, with i, j being their respective generation indices. Here Q_L (L_L) is the SM left-handed quark (lepton) doublet whereas d_R (l_R) is the right-handed down quark (lepton) singlet. The Lagrangian in Eq. 10 is written in

the weak basis of the fermionic fields. Transforming into the mass basis and using the Fierz identities, we can obtain relations between the LQ couplings and the NP WCs of $b \rightarrow c\tau\bar{\nu}$ transitions. Thus, one can obtain the following relations

$$\begin{aligned} C_{V_L}^{b \rightarrow c} &= \frac{1}{2\sqrt{2}G_F V_{cb}} \sum_{k=1}^3 V_{k3} \frac{h_L^{23} h_L^{k3*}}{M_{U_1}^2} \simeq \frac{1}{2\sqrt{2}G_F V_{cb}} V_{33} \frac{h_L^{23} h_L^{33*}}{M_{U_1}^2}, \\ C_{S_R}^{b \rightarrow c} &= -\frac{1}{2\sqrt{2}G_F V_{cb}} \sum_{k=1}^3 V_{k3} \frac{2h_L^{23} h_R^{k3*}}{M_{U_1}^2} \simeq -\frac{1}{2\sqrt{2}G_F V_{cb}} V_{33} \frac{2h_L^{23} h_R^{33*}}{M_{U_1}^2}, \end{aligned} \quad (11)$$

where V_{k3} is the CKM matrix elements and M_{U_1} is the mass of the LQ, which is assumed to be 1 TeV in this analysis. To get the final expressions, we neglect the terms containing V_{13} and V_{23} as they are Cabibbo suppressed. For $b \rightarrow u\tau\bar{\nu}$ transition, the relations in Eq. 11 can be written as

$$\begin{aligned} C_{V_L}^{b \rightarrow u} &= \frac{1}{2\sqrt{2}G_F V_{ub}} V_{33} \frac{h_L^{13} h_L^{33*}}{M_{U_1}^2}, \\ C_{S_R}^{b \rightarrow u} &= -\frac{1}{2\sqrt{2}G_F V_{ub}} V_{33} \frac{2h_L^{13} h_R^{33*}}{M_{U_1}^2}. \end{aligned} \quad (12)$$

This LQ can also generate the interaction terms for $b \rightarrow s\mu^+\mu^-$ transition. The NP WCs in $b \rightarrow s\mu^+\mu^-$ can be expressed in terms of the LQ couplings as

$$C_9^{\text{NP}} = -C_{10}^{\text{NP}} = \frac{\pi}{\sqrt{2}G_F V_{tb} V_{ts}^* \alpha_{em}} \frac{h_L^{22} h_L^{32*}}{M_{U_1}^2}. \quad (13)$$

This particular choice is motivated from the global fit of $b \rightarrow s\mu^+\mu^-$ data. From the global fit [37], $C_9^{\text{NP}} = -C_{10}^{\text{NP}}$ is the only solution which can be addressed by U_1 LQ scenario.

IV. FIT METHODOLOGY AND RESULTS

In this section, we describe the details of our fitting procedure to determine the LQ couplings h_L^{13} and h_R^{33} for $b \rightarrow u\tau\bar{\nu}$ transition. We assume the value of h_L^{33} to be 1 because of the hierarchy in coupling constants of left-chiral particles in flavor basis. We also assume these couplings to be real. To obtain the values of h_L^{13} and h_R^{33} , we perform a χ^2 analysis by using the CERN minimization code MINUIT [67, 68]. In doing so, we use the data from $b \rightarrow c\tau\bar{\nu}$, $b \rightarrow s\mu^+\mu^-$ and $b \rightarrow u\tau\bar{\nu}$ transition processes. Thus, the total χ^2 is expressed as

$$\chi_{\text{total}}^2 = \chi_{b \rightarrow c\tau\bar{\nu}}^2 + \chi_{b \rightarrow s\mu^+\mu^-}^2 + \chi_{b \rightarrow u\tau\bar{\nu}}^2. \quad (14)$$

Below we provide the discussion about the individual χ^2 function in detail.

In $b \rightarrow c\tau\bar{\nu}$ sector, we take the current data of R_D , R_{D^*} , $R_{J/\psi}$ and $F_L^{D^*}$ in our fit. We do not include measurement of the τ polarization in $B \rightarrow D^*\tau\bar{\nu}$ decay because of its large statistical uncertainty [5]. Therefore, the χ^2 function for this sector looks as follows

$$\chi_{b \rightarrow c\tau\bar{\nu}}^2 = \sum_{R_D, R_{D^*}, R_{J/\psi}, F_L^{D^*}} (O^{\text{th}}(C_i^{b \rightarrow c}) - O^{\text{exp}}) \mathcal{C}^{-1} (O^{\text{th}}(C_i^{b \rightarrow c}) - O^{\text{exp}}), \quad (15)$$

where $O^{\text{th}}(C_i^{b \rightarrow c})$ are NP predictions of each observable and O^{exp} are the corresponding experimental central values. Here \mathcal{C} denotes the covariance matrix which includes both theory and experimental correlations. We also include the constraint from the branching fraction of $B_c \rightarrow \tau\bar{\nu}$. We set the upper limit of this quantity to be 30% which is calculated from the lifetime of B_c meson [69].

In the context of U_1 LQ, the NP WCs in $b \rightarrow s\mu^+\mu^-$ transition are related as $C_9^{\text{NP}} = -C_{10}^{\text{NP}} = -0.53 \pm 0.09$ [37]. Hence, we can use this result to constrain the LQ couplings. For this sector, we define the χ^2 function as

$$\chi_{b \rightarrow s\mu^+\mu^-}^2 = \left(\frac{C_9^{\text{NP}} - (-0.53)}{0.09} \right)^2. \quad (16)$$

In $b \rightarrow u\tau\bar{\nu}$ transition, the only measured quantity is the branching fraction of $B^+ \rightarrow \tau^+\nu$ process with a value $(1.09 \pm 0.24) \times 10^{-4}$ [66]. The SM prediction for this branching ratio is $(8.80 \pm 0.73) \times 10^{-5}$. Therefore, there is a tension between the measured value and the SM prediction at the level of $\sim 1\sigma$. In addition, Belle collaboration has put an upper limit on the branching fraction of $B \rightarrow \pi^-\tau^+\nu$. They obtained an upper limit of 2.5×10^{-4} at the 90% C.L. [70]. Therefore, the χ^2 function for this sector can be written as

$$\chi_{b \rightarrow u\tau\bar{\nu}}^2 = \frac{(\text{Br}(B^+ \rightarrow \tau^+\nu) - 1.09 \times 10^{-4})^2}{(0.24 \times 10^{-4})^2 + (0.73 \times 10^{-5})^2} + \frac{(\text{Br}(B \rightarrow \pi^-\tau^+\nu) - 1.25 \times 10^{-4})^2}{(0.76 \times 10^{-4})^2}. \quad (17)$$

In writing the χ^2 term for the branching fraction of $B \rightarrow \pi^-\tau^+\nu$, we have adjusted the central value and the error such that we can get the value of upper limit at a level of 1.645σ (or 90% C.L.).

We use the `Flavio` package [71] to compute the observables which are taken into the fit. Minimizing the χ_{total}^2 , we obtain the best fit values $h_L^{13} = 0.03$ and $h_R^{33} = 0.04$ of the LQ couplings for $b \rightarrow u\tau\bar{\nu}$ transition. We find the correlation between these two parameters is ~ 0.80 . We also determine the 1σ allowed parameter space for h_L^{13} - h_R^{33} . This is shown in Fig. 1. This figure shows space for NP in $b \rightarrow u$ transition allowed by current data in B sector.

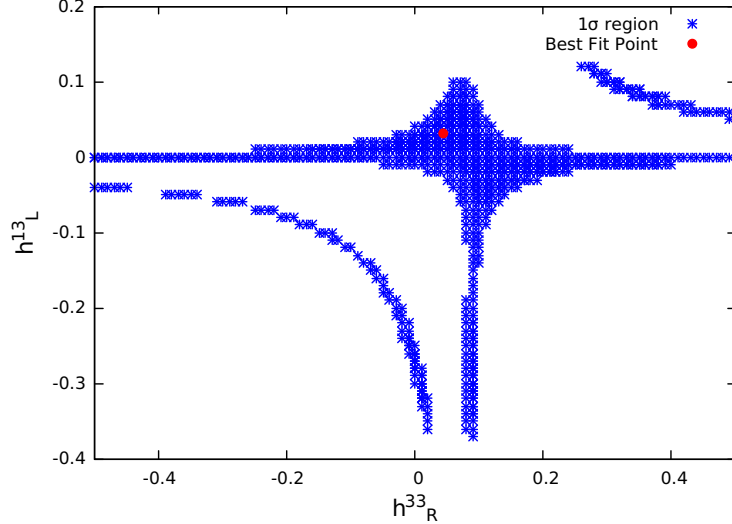


FIG. 1: 1σ allowed region in the $h_L^{13} - h_R^{33}$ plane, constrained by the current data from B sector.

V. PREDICTIONS FOR $b \rightarrow u\tau\bar{\nu}$ DECAY OBSERVABLES IN U_1 LQ

In this section, we investigate the effects of U_1 LQ on various decay modes mediated by $b \rightarrow u\tau\bar{\nu}$ transition. In particular, we focus on the decays $B \rightarrow \pi\tau\bar{\nu}$, $B \rightarrow (\rho, \omega)\tau\bar{\nu}$ and $B_s \rightarrow (K, K^*)\tau\bar{\nu}$. We mainly focus on the branching fraction and the lepton flavor ratio $R^{\tau/\ell}$ for each decay. In addition, we compute the standard angular observables, e.g., the forward-backward asymmetry A_{FB} , the τ polarization fraction P_τ and the longitudinal polarization fraction of vector meson F_L , for each decay mode. These observables are defined as follows

$$\begin{aligned} \frac{d\text{Br}}{dq^2} &= \frac{d\Gamma/dq^2}{\Gamma_{\text{total}}}, & R_{P,V}^{\tau/\ell}(q^2) &= \frac{d\Gamma(B \rightarrow (P, V)\tau\bar{\nu})/dq^2}{d\Gamma(B \rightarrow (P, V)\ell\bar{\nu})/dq^2}, \\ P_\tau(q^2) &= \frac{d\Gamma^{\lambda_\tau=1/2}/dq^2 - d\Gamma^{\lambda_\tau=-1/2}/dq^2}{d\Gamma^{\lambda_\tau=1/2}/dq^2 + d\Gamma^{\lambda_\tau=-1/2}/dq^2}, & F_L(q^2) &= \frac{d\Gamma^{\lambda_V=0}/dq^2}{d\Gamma/dq^2}, \\ A_{FB}(q^2) &= \frac{1}{d\Gamma/dq^2} \left[\int_0^1 \frac{d^2\Gamma}{dq^2 d\cos\theta_\tau} d\cos\theta_\tau - \int_{-1}^0 \frac{d^2\Gamma}{dq^2 d\cos\theta_\tau} d\cos\theta_\tau \right]. \end{aligned} \quad (18)$$

Here, $d\Gamma^{\lambda_\tau=\pm 1/2}/dq^2$ are the differential decay rates of $B \rightarrow (P, V)$ processes with the polarization of the τ lepton $\lambda_\tau = \pm 1/2$ whereas $d\Gamma^{\lambda_V=0}/dq^2$ is the decay rate of $B \rightarrow V$ decay with the polarization of vector V meson $\lambda_V = 0$. In the U_1 LQ model, the differential decay

rates for $B \rightarrow (P, V)\tau\bar{\nu}$ decays are written as [72]

$$\begin{aligned} \frac{d\Gamma(B \rightarrow P\tau\bar{\nu})}{dq^2} &= \frac{G_F^2 |V_{ub}|^2}{192\pi^3 m_B^3} q^2 \sqrt{\lambda_P(q^2)} \left(1 - \frac{m_\tau^2}{q^2}\right)^2 \times \\ &\quad \left[|1 + C_{V_L}^{b \rightarrow u}|^2 \left[\left(1 + \frac{m_\tau^2}{2q^2}\right) H_{V,0}^{s2} + \frac{3m_\tau^2}{2q^2} H_{V,t}^{s2} \right] \right. \\ &\quad \left. + \frac{3}{2} |C_{S_R}^{b \rightarrow u}|^2 H_S^{s2} + 3 \operatorname{Re} \left[(1 + C_{V_L}^{b \rightarrow u}) C_{S_R}^{*b \rightarrow u} \right] \frac{m_\tau}{\sqrt{q^2}} H_S^s H_{V,t}^s \right], \end{aligned} \quad (19)$$

and

$$\begin{aligned} \frac{d\Gamma(B \rightarrow V\tau\bar{\nu})}{dq^2} &= \frac{G_F^2 |V_{ub}|^2}{192\pi^3 m_B^3} q^2 \sqrt{\lambda_V(q^2)} \left(1 - \frac{m_\tau^2}{q^2}\right)^2 \times \\ &\quad \left[(|1 + C_{V_L}^{b \rightarrow u}|^2) \left[\left(1 + \frac{m_\tau^2}{2q^2}\right) (H_{V,+}^2 + H_{V,-}^2 + H_{V,0}^2) + \frac{3m_\tau^2}{2q^2} H_{V,t}^2 \right] \right. \\ &\quad \left. + \frac{3}{2} |C_{S_R}^{b \rightarrow u}|^2 H_S^2 + 3 \operatorname{Re} \left[(1 + C_{V_L}^{b \rightarrow u}) C_{S_R}^{*b \rightarrow u} \right] \frac{m_\tau}{\sqrt{q^2}} H_S H_{V,t} \right], \end{aligned} \quad (20)$$

with

$$\lambda_{P,V}(q^2) = ((m_B - m_{P,V})^2 - q^2) ((m_B + m_{P,V})^2 - q^2). \quad (21)$$

The SM decay rate for μ/e lepton can be obtained by setting the NP WCs to zero and by replacing m_τ with mass of μ/e . The nonzero helicity amplitudes of $B \rightarrow P$ processes can be expressed in terms of the two form factors $F_{0,+}(q^2)$, characterizing $B \rightarrow P$ transitions and are given as

$$H_{V,0}^s(q^2) = \sqrt{\frac{\lambda_P(q^2)}{q^2}} F_+(q^2), \quad H_{V,t}^s(q^2) = \frac{m_B^2 - m_P^2}{\sqrt{q^2}} F_0(q^2), \quad H_S^s(q^2) = \frac{m_B^2 - m_P^2}{m_b - m_u} F_0(q^2). \quad (22)$$

On the other hand, the non-zero helicity amplitudes for $B \rightarrow V$ transitions can be expressed in terms of the corresponding hadronic form factors as

$$\begin{aligned} H_{V,\pm}(q^2) &= (m_B + m_V) A_1(q^2) \mp \frac{\sqrt{\lambda_V(q^2)}}{m_B + m_V} V(q^2), \\ H_{V,0}(q^2) &= \frac{m_B + m_V}{2m_V \sqrt{q^2}} \left[-(m_B^2 - m_V^2 - q^2) A_1(q^2) + \frac{\lambda_V(q^2)}{(m_B + m_V)} A_2(q^2) \right], \\ H_{V,t}(q^2) &= -\sqrt{\frac{\lambda_V(q^2)}{q^2}} A_0(q^2), \\ H_S(q^2) &= -\frac{\sqrt{\lambda_V(q^2)}}{m_b + m_u} A_0(q^2). \end{aligned} \quad (23)$$

All these form-factors are calculated using different techniques for different decay modes. We will discuss them individually for each case in the following subsections. The decay distributions for the τ lepton polarizations $\lambda = \pm 1/2$ in $B \rightarrow P \tau \bar{\nu}$ decay are given by

$$\begin{aligned} \frac{d\Gamma^{\lambda\tau=1/2}(B \rightarrow P\tau\bar{\nu})}{dq^2} &= \frac{G_F^2|V_{ub}|^2}{192\pi^3m_B^3}q^2\sqrt{\lambda_P(q^2)}\left(1-\frac{m_\tau^2}{q^2}\right)^2 \times \\ &\quad \left[\frac{1}{2}|1+C_{V_L}^{b\rightarrow u}|^2\frac{m_\tau^2}{q^2}(H_{V,0}^{s2}+3H_{V,t}^{s2})+\frac{3}{2}|C_{S_R}^{b\rightarrow u}|^2H_S^{s2}\right. \\ &\quad \left.+3\text{Re}[(1+C_{V_L}^{b\rightarrow u})C_{S_R}^{*b\rightarrow u}]\frac{m_\tau}{\sqrt{q^2}}H_S^sH_{V,t}^s\right], \\ \frac{d\Gamma^{\lambda\tau=-1/2}(B \rightarrow P\tau\bar{\nu})}{dq^2} &= \frac{G_F^2|V_{ub}|^2}{192\pi^3m_B^3}q^2\sqrt{\lambda_P(q^2)}\left(1-\frac{m_\tau^2}{q^2}\right)^2 \times |1+C_{V_L}^{b\rightarrow u}|^2H_{V,0}^{s2}. \end{aligned} \quad (24)$$

These distributions for $B \rightarrow V\tau\bar{\nu}$ decays are expressed as follows

$$\begin{aligned} \frac{d\Gamma^{\lambda\tau=1/2}(B \rightarrow V\tau\bar{\nu})}{dq^2} &= \frac{G_F^2|V_{ub}|^2}{192\pi^3m_B^3}q^2\sqrt{\lambda_V(q^2)}\left(1-\frac{m_\tau^2}{q^2}\right)^2 \times \\ &\quad \left[\frac{1}{2}(|1+C_{V_L}^{b\rightarrow u}|^2)\frac{m_\tau^2}{q^2}(H_{V,+}^2+H_{V,-}^2+H_{V,0}^2+3H_{V,t}^2)\right. \\ &\quad \left.+\frac{3}{2}|C_{S_R}^{b\rightarrow u}|^2H_S^2+3\text{Re}[(1+C_{V_L}^{b\rightarrow u})(C_{S_R}^{*b\rightarrow u})]\frac{m_\tau}{\sqrt{q^2}}H_S H_{V,t}\right], \\ \frac{d\Gamma^{\lambda\tau=-1/2}(B \rightarrow V\tau\bar{\nu})}{dq^2} &= \frac{G_F^2|V_{ub}|^2}{192\pi^3m_B^3}q^2\sqrt{\lambda_V(q^2)}\left(1-\frac{m_\tau^2}{q^2}\right)^2 \times \\ &\quad [(|1+C_{V_L}^{b\rightarrow u}|^2)(H_{V,+}^2+H_{V,-}^2+H_{V,0}^2)] \end{aligned} \quad (25)$$

The decay distribution of $B \rightarrow (P, V)\tau\bar{\nu}$ transitions with respect to q^2 and θ_τ can be written as

$$\frac{d^2\Gamma(B \rightarrow (P, V)\tau\bar{\nu})}{dq^2 d\cos\theta} = a_\theta^{P,V}(q^2) + b_\theta^{P,V}(q^2)\cos\theta + c_\theta^{P,V}(q^2)\cos^2\theta. \quad (26)$$

The definition of A_{FB} in Eq. 18 leads to the forward-backward asymmetry to be

$$A_{FB}(q^2) = \frac{1}{(d\Gamma/dq^2)}b_\theta^{P,V}(q^2), \quad (27)$$

where $b_\theta^{P,V}$ are given by

$$\begin{aligned} b_\theta^P(q^2) &= \frac{G_F^2|V_{ub}|^2}{128\pi^3m_B^3}q^2\sqrt{\lambda_P(q^2)}\left(1-\frac{m_\tau^2}{q^2}\right)^2 \times \\ &\quad \left[|1+C_{V_L}^{b\rightarrow u}|^2\frac{m_\tau^2}{q^2}H_{V,0}^sH_{V,t}^s+\text{Re}[(1+C_{V_L}^{b\rightarrow u})C_{S_R}^{*b\rightarrow u}]\frac{m_\tau}{\sqrt{q^2}}H_S^sH_{V,t}^s\right], \end{aligned} \quad (28)$$

and

$$b_\theta^V = \frac{G_F^2 |V_{ub}|^2}{128\pi^3 m_B^3} q^2 \sqrt{\lambda_V(q^2)} \left(1 - \frac{m_\tau^2}{q^2}\right)^2 \left[\frac{1}{2} (|1 + C_{V_L}^{b \rightarrow u}|^2) (H_{V,+}^2 - H_{V,-}^2) \right. \\ \left. + |1 + C_{V_L}^{b \rightarrow u}|^2 \frac{m_\tau^2}{q^2} H_{V,0} H_{V,t} + \text{Re} [(1 + C_{V_L}^{b \rightarrow u}) C_{S_R}^{*b \rightarrow u}] \frac{m_\tau}{\sqrt{q^2}} H_S H_{V,0} \right]. \quad (29)$$

The differential decay rate with the longitudinally polarized V meson $d\Gamma^{\lambda_V=0}/dq^2$ can be written as

$$\frac{d\Gamma^{\lambda_V=0}}{dq^2} = \frac{G_F^2 |V_{ub}|^2}{192\pi^3 m_B^3} q^2 \sqrt{\lambda_V(q^2)} \left(1 - \frac{m_\tau^2}{q^2}\right)^2 \times \\ \left[|1 + C_{V_L}^{b \rightarrow u}|^2 \left[\left(1 + \frac{m_\tau^2}{2q^2}\right) H_{V,0}^2 + \frac{3m_\tau^2}{2q^2} H_{V,t}^2 \right] \right. \\ \left. + \frac{3}{2} |C_{S_R}^{b \rightarrow u}|^2 H_S^2 + 3\text{Re} [(1 + C_{V_L}^{b \rightarrow u}) C_{S_R}^{*b \rightarrow u}] \frac{m_\tau}{\sqrt{q^2}} H_S H_{V,t} \right]. \quad (30)$$

After collating all the required information about various observables, we now proceed to appraise their values for various decay modes.

A. $B \rightarrow \pi\tau\bar{\nu}$ decay:

The form-factors F_0 and F_1 for this process are computed by lattice QCD approach, which are parametrized as follows [73]

$$F_+(q^2) = \frac{1}{1 - q^2/m_{B^*}^2} \sum_{n=0}^{N-1} b_n^+ \left[z^n - (-1)^{n-N} \frac{n}{N} z^N \right], \quad F_0(q^2) = \sum_{n=0}^{N-1} b_n^0 z^n, \quad (31)$$

where $z(q^2) = \frac{\sqrt{t_+ - q^2} - \sqrt{t_+ - t_0}}{\sqrt{t_+ - q^2} + \sqrt{t_+ - t_0}}$, $t_+ = (M_B + M_\pi)^2$, $t_0 = (M_B + M_\pi) (\sqrt{M_B} - \sqrt{M_\pi})^2$, $N = 4$ and $m_{B^*} = 5.6794(10)$ GeV. The inputs of these form-factors are given by [73]

$$b_0^+ = 0.419(13), \quad b_1^+ = -0.495(54), \quad b_2^+ = -0.43(13), \quad b_3^+ = 0.22(0.31), \\ b_0^0 = 0.510(19), \quad b_1^0 = -1.700(82), \quad b_2^0 = 1.53(19), \quad b_3^0 = 4.52(0.83). \quad (32)$$

Using these form-factors, we estimate the values of the branching fraction, $R_\pi^{\tau/\ell}$, P_τ and A_{FB} , for this decay mode both in the SM as well as in the U_1 LQ model. The variation of these observables as a function of q^2 are shown in Fig. 2. From the plots, one can notice that the impact of U_1 LQ on the branching fraction as well as on the lepton non-universality parameter $R_\pi^{\tau/\ell}$ is quite significant whereas its effect is rather minimal on the τ

polarization P_τ as well as on forward backward asymmetry A_{FB} . The predicted values of these observables both in the SM as well as in LQ scenario are listed in Table I. Since the discrepancy between the SM and the LQ model predictions for the $R_\pi^{\tau/\ell}$ value is fairly large, it should be searched for at LHCb or Belle II experiments.

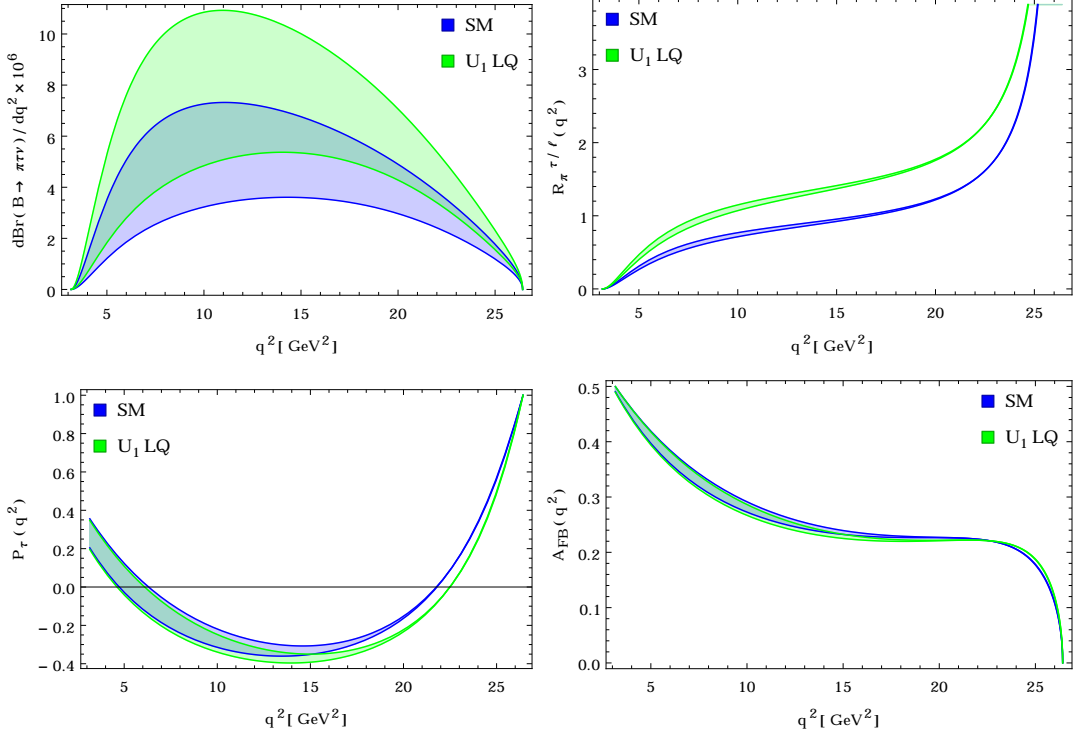


FIG. 2: Variation of branching fraction (top-left panel), $R_\pi^{\tau/\ell}$ (top-right panel), P_τ (bottom-left panel) and A_{FB} (bottom-right panel) with respect to q^2 for $B \rightarrow \pi\tau\bar{\nu}$ process.

	$\text{Br}(B \rightarrow \pi\tau\bar{\nu})$	$R_\pi^{\tau/\ell}$	P_τ	A_{FB}
SM	$(0.847 \pm 0.165) \times 10^{-4}$	0.634 ± 0.041	-0.175 ± 0.053	0.262 ± 0.007
U_1 LQ	$(1.244 \pm 0.242) \times 10^{-4}$	0.921 ± 0.057	-0.236 ± 0.051	0.257 ± 0.008

TABLE I: Predicted values of various observables for $B \rightarrow \pi\tau\bar{\nu}$ process, both in the SM and LQ model.

B. $B \rightarrow (\rho, \omega)\tau\bar{\nu}$ decays:

The form-factors for $B \rightarrow (\rho, \omega)\tau\bar{\nu}$ decay are determined by light cone sum rule (LCSR) technique [74], which are parametrized as

$$F_i(q^2) = (1 - q^2/m_{R,i}^2)^{-1} \sum_{k=0} a_k^i [z(q^2) - z(0)]^k, \quad (33)$$

where $z(q^2) = \frac{\sqrt{t_+ - q^2} - \sqrt{t_+ - t_0}}{\sqrt{t_+ - q^2} + \sqrt{t_+ - t_0}}$, $t_{\pm} = (M_B \pm M_{\rho,\omega})^2$ and $t_0 = t_+(1 - \sqrt{1 - t_-/t_+})$. Here the form-factors F_i refer to $V(q^2)$, $A_0(q^2)$, $A_1(q^2)$ and $A_{12}(q^2)$, where $A_{12}(q^2)$ is defined as

$$A_{12}(q^2) = \frac{(M_B + M_{\rho,\omega})^2 (M_B^2 - M_{\rho,\omega}^2 - q^2) A_1(q^2) - \lambda_{\rho,\omega} A_2(q^2)}{16M_B M_{\rho,\omega}^2 (M_B + M_{\rho,\omega})}. \quad (34)$$

The values of the resonance masses in Eq. (33) are considered as $m_{R,V} = 5.325$ GeV, $m_{R,A_0} = 5.279$ GeV, $m_{R,A_1} = 5.724$ GeV and $m_{R,A_{12}} = 5.724$ GeV for both the decays. The inputs of the form-factors for $B \rightarrow \rho$ decay are [74]

$$\begin{aligned} a_0^V &= 0.33(3), & a_1^V &= -0.86(18), & a_2^V &= 1.80(97), & a_0^{A_0} &= 0.36(4), & a_1^{A_0} &= -0.83(20), \\ a_2^{A_0} &= 1.33(1.05), & a_0^{A_1} &= 0.26(3), & a_1^{A_1} &= 0.39(14), & a_2^{A_1} &= 0.16(41), \\ a_0^{A_{12}} &= 0.30(3), & a_1^{A_{12}} &= 0.76(20), & a_2^{A_{12}} &= 0.46(76), \end{aligned} \quad (35)$$

whereas those for $B \rightarrow \omega$ decay are [74]

$$\begin{aligned} a_0^V &= 0.30(4), & a_1^V &= -0.83(29), & a_2^V &= 1.72(1.24), & a_0^{A_0} &= 0.33(5), & a_1^{A_0} &= -0.83(30), \\ a_2^{A_0} &= 1.42(1.25), & a_0^{A_1} &= 0.24(3), & a_1^{A_1} &= 0.34(24), & a_2^{A_1} &= 0.09(57), \\ a_0^{A_{12}} &= 0.27(4), & a_1^{A_{12}} &= 0.66(26), & a_2^{A_{12}} &= 0.28(98). \end{aligned} \quad (36)$$

We use these form-factors in our computation and calculate the branching fraction, $R_{\rho,\omega}^{\tau/\ell}$, P_{τ} , A_{FB} and F_L observables for both the decays. In Figs. 3 and 4, we plot these observables as a function of q^2 for $B \rightarrow \rho\tau\bar{\nu}$ and $B \rightarrow \omega\tau\bar{\nu}$ respectively. The computed average values of these observables for both decays are listed in Tables II and III respectively. Analogous to $B \rightarrow \pi\tau\bar{\nu}$ mode, in this case also, i.e., for both the decay modes, the branching fractions as well as the lepton non-universality parameters $R_{\rho,\omega}^{\tau/\ell}$ deviate significantly from their SM predictions due to the LQ effect whereas the observables P_{τ} , A_{FB} and F_L are almost consistent with their SM estimations.

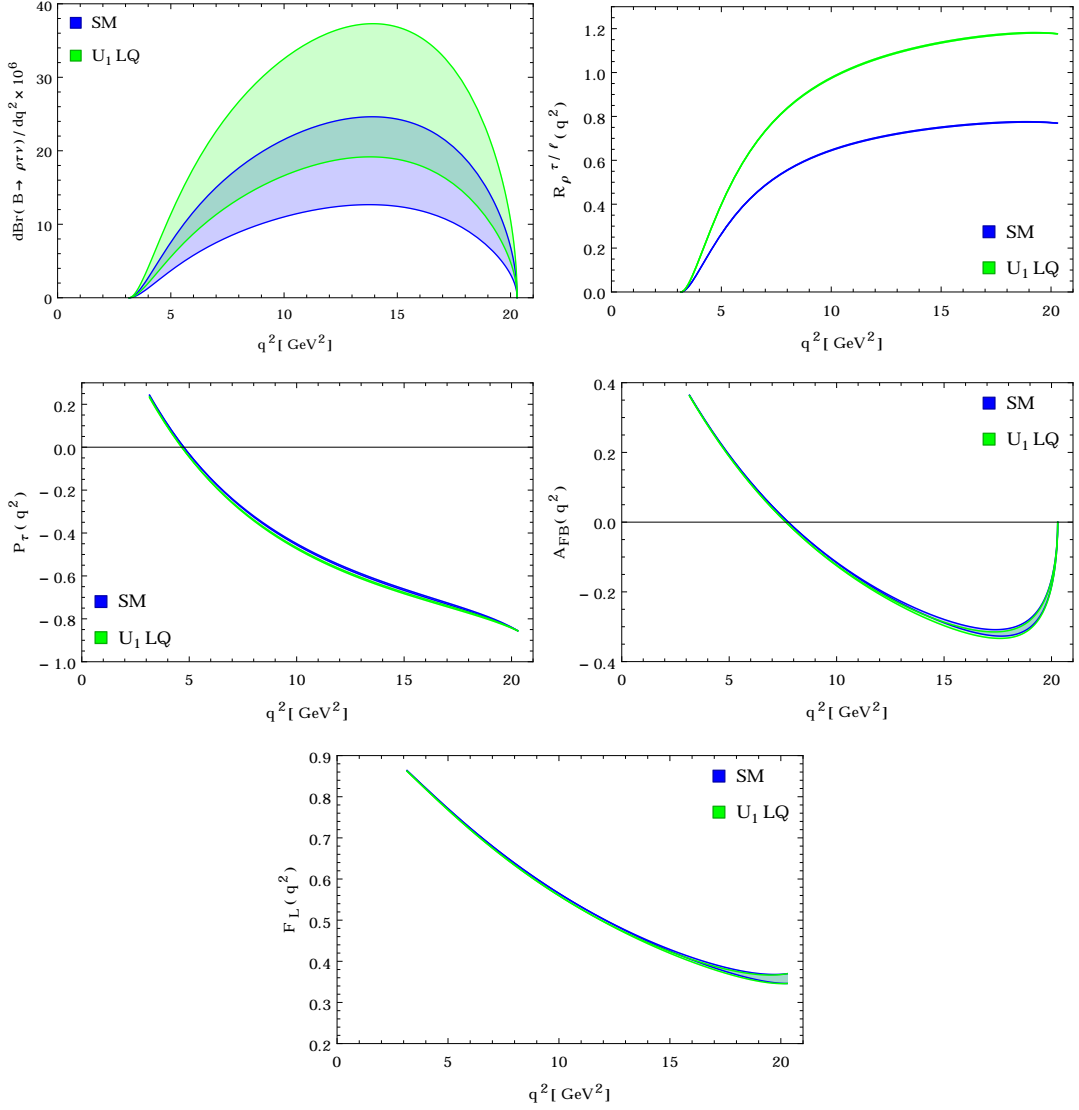


FIG. 3: The q^2 variation of differential branching fraction, $R_\rho^{\tau/\ell}$, P_τ , A_{FB} and F_L observables for $B \rightarrow \rho\tau\bar{\nu}$ process in the SM as well as in U_1 LQ model.

	$\text{Br}(B \rightarrow \rho\tau\bar{\nu})$	$R_\rho^{\tau/\ell}$	P_τ	A_{FB}	F_L
SM	$(2.165 \pm 0.545) \times 10^{-4}$	0.526 ± 0.021	-0.540 ± 0.056	-0.174 ± 0.060	0.504 ± 0.086
U_1 LQ	$(3.277 \pm 0.828) \times 10^{-4}$	0.796 ± 0.031	-0.556 ± 0.053	-0.181 ± 0.060	0.500 ± 0.087

TABLE II: Predicted values of various observables for $B \rightarrow \rho\tau\bar{\nu}$ decay mode both in the SM as well as in LQ model.

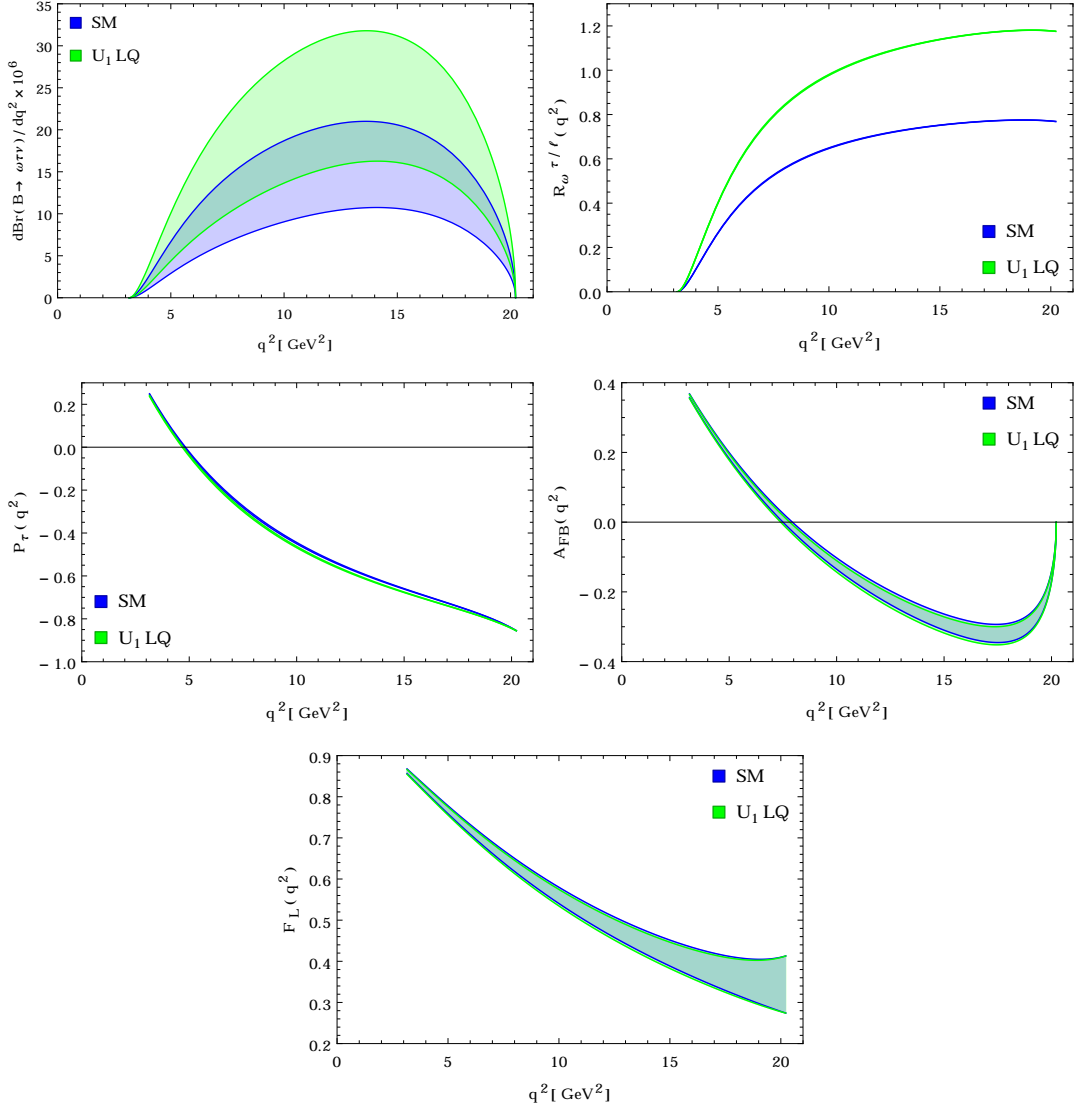


FIG. 4: Variation of differential branching fraction, $R_\omega^{\tau/\ell}$, P_τ , A_{FB} and F_L observables with respect to q^2 for $B \rightarrow \omega\tau\bar{\nu}$ process.

	$\text{Br}(B \rightarrow \omega\tau\bar{\nu})$	$R_\omega^{\tau/\ell}$	P_τ	A_{FB}	F_L
SM	$(1.828 \pm 0.554) \times 10^{-4}$	0.529 ± 0.031	-0.535 ± 0.080	-0.175 ± 0.085	0.500 ± 0.120
U_1 LQ	$(2.765 \pm 0.843) \times 10^{-4}$	0.800 ± 0.046	-0.552 ± 0.075	-0.183 ± 0.085	0.495 ± 0.122

TABLE III: Predictions for various observables of $B \rightarrow \omega\tau\bar{\nu}$ decay in the SM as well as in the U_1 LQ model.

C. $B_s \rightarrow (K, K^*)\tau\bar{\nu}$ decays:

The form-factors of $B_s \rightarrow K$ transition are determined in lattice QCD technique. In this approach, the two relevant form-factors are parametrized as follows [75]

$$\begin{aligned} F_+(q^2) &= (1 - q^2/m_{B^{*+}}^2)^{-1} \sum_{k=0}^{K-1} b_k^+ \left[z^k - (-1)^{k-K} \frac{k}{K} z^K \right], \\ F_0(q^2) &= (1 - q^2/m_{B^{*0}}^2)^{-1} \sum_{k=0}^{K-1} b_k^0 z^k, \end{aligned} \quad (37)$$

where $z(q^2) = \frac{\sqrt{t_{\text{cut}} - q^2} - \sqrt{t_{\text{cut}} - t_0}}{\sqrt{t_{\text{cut}} - q^2} + \sqrt{t_{\text{cut}} - t_0}}$, $m_{B^{*+}} = 5.32465$ GeV, $m_{B^{*0}} = 5.68$ GeV, $\sqrt{t_{\text{cut}}} = 5.414$ GeV, $t_0 = t_{\text{cut}} - \sqrt{t_{\text{cut}}(t_{\text{cut}} - t_-)}$ and $t_- = (M_{B_s} - M_K)^2$. The values of the input parameters in the above mentioned form-factors are as follows [75]

$$\begin{aligned} b_0^+ &= 0.3623(0.0178), & b_1^+ &= -0.9559(0.1307), & b_2^+ &= -0.8525(0.4783), \\ b_3^+ &= 0.2785(0.6892), & b_0^0 &= 0.1981(0.0101), & b_1^0 &= -0.1661(0.1130), \\ b_2^0 &= -0.6430(0.4385), & b_3^0 &= -0.3754(0.4535). \end{aligned} \quad (38)$$

With these values, we calculate the branching fraction, $R_K^{\tau/\ell}$, P_τ and A_{FB} of $B_s \rightarrow K\tau\bar{\nu}$ decay for the SM and for the U_1 LQ model. In Fig. 5, we plot these quantities as a function of q^2 and also listed their predicted values in Table IV. In this case the branching fraction and the P_τ observables have mild deviation from their SM values due to the effect of U_1 LQ whereas discrepancy between SM and LQ predicted values for $R_K^{\tau/\ell}$ observable is considerably large. On the other hand the forward-backward asymmetry parameter remains consistent with its SM value in the LQ scenario.

	$\text{Br}(B_s \rightarrow K\tau\bar{\nu})$	$R_K^{\tau/\ell}$	P_τ	A_{FB}
SM	$(0.765 \pm 0.155) \times 10^{-4}$	0.767 ± 0.073	-0.244 ± 0.060	0.253 ± 0.007
U_1 LQ	$(1.129 \pm 0.230) \times 10^{-4}$	1.133 ± 0.104	-0.290 ± 0.057	0.248 ± 0.008

TABLE IV: Predicted values of the observables for $B_s \rightarrow K\tau\bar{\nu}$ decay process in both the SM and the LQ model.

For $B_s \rightarrow K^*\tau\bar{\nu}$ decay process, we use the form-factors calculated using lattice QCD approach, which are expressed as [76]

$$F(q^2) = \frac{1}{P(q^2; \Delta m)} [a_0 + a_1 z(q^2)], \quad (39)$$

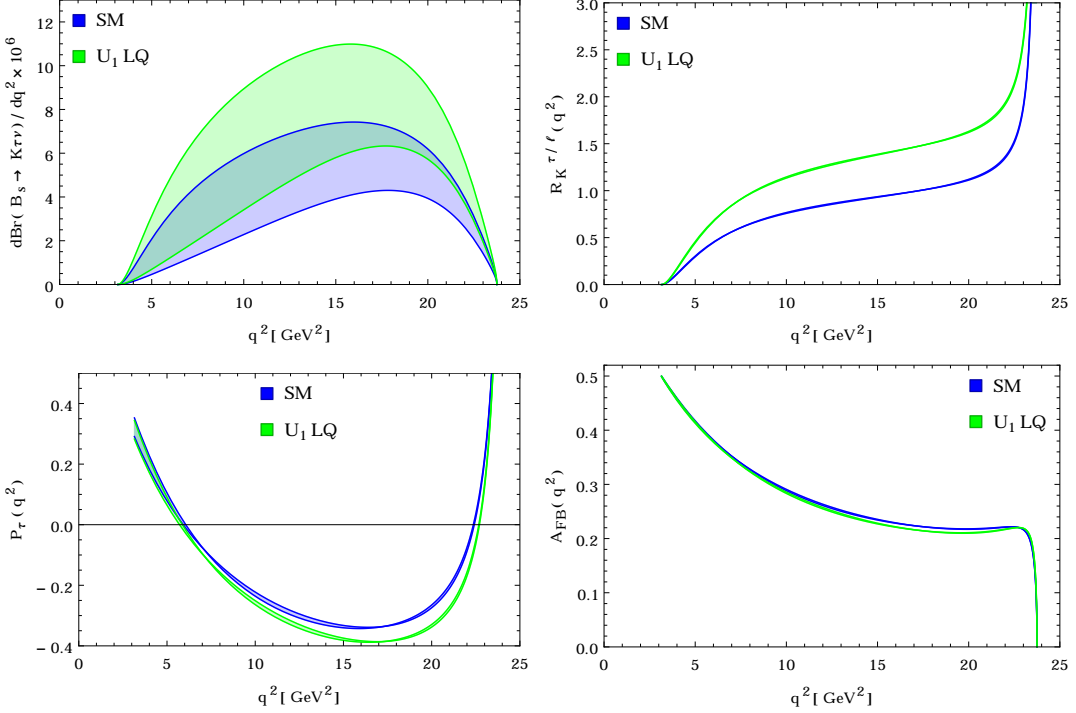


FIG. 5: The q^2 variation plots for the branching fraction, $R_K^{\tau/\ell}$, P_τ and A_{FB} of $B_s \rightarrow K\tau\bar{\nu}$ decay.

where F refers to the form-factors $V(q^2)$, $A_0(q^2)$, $A_1(q^2)$ and $A_{12}(q^2)$. The expression of $A_{12}(q^2)$ is the same as that of Eq. 34. Here $P(q^2; \Delta m) = 1 - q^2 / (M_{B_s} + \Delta m)^2$ where $\Delta m = -87$ MeV for $A_0(q^2)$, $\Delta m = -42$ MeV for $V(q^2)$ and $\Delta m = 350$ MeV for $A_1(q^2)$ and $A_{12}(q^2)$. The expansion parameter is defined as $z(q^2) = \frac{\sqrt{t_+ - q^2} - \sqrt{t_+ - t_0}}{\sqrt{t_+ - q^2} + \sqrt{t_+ - t_0}}$, where $t_0 = 12$ GeV and $t_\pm = (M_{B_s} \pm M_{K^*})^2$. The input parameters of the form-factors are given by [76]

$$\begin{aligned}
a_0^V &= 0.322(0.048), & a_1^V &= -3.04(0.67), & a_0^{A_0} &= 0.476(0.042), \\
a_1^{A_0} &= -2.29(0.74), & a_0^{A_1} &= 0.2342(0.0122), & a_1^{A_1} &= 0.100(0.174), \\
a_0^{A_{12}} &= 0.1954(0.0133), & a_1^{A_{12}} &= 0.350(0.190). & &
\end{aligned} \tag{40}$$

We calculate the branching fraction, $R_{K^*}^{\tau/\ell}$, P_τ , A_{FB} and F_L for $B_s \rightarrow K^*\tau\bar{\nu}$ decay in the SM as well as in the U_1 LQ model. We plot these observables as a function of q^2 as shown in Fig. 6. We also compute their average values and list them in Table V. For this process also the LQ effect is significant only for branching fraction and the lepton non-universality parameter $R_{K^*}^{\tau/\ell}$.

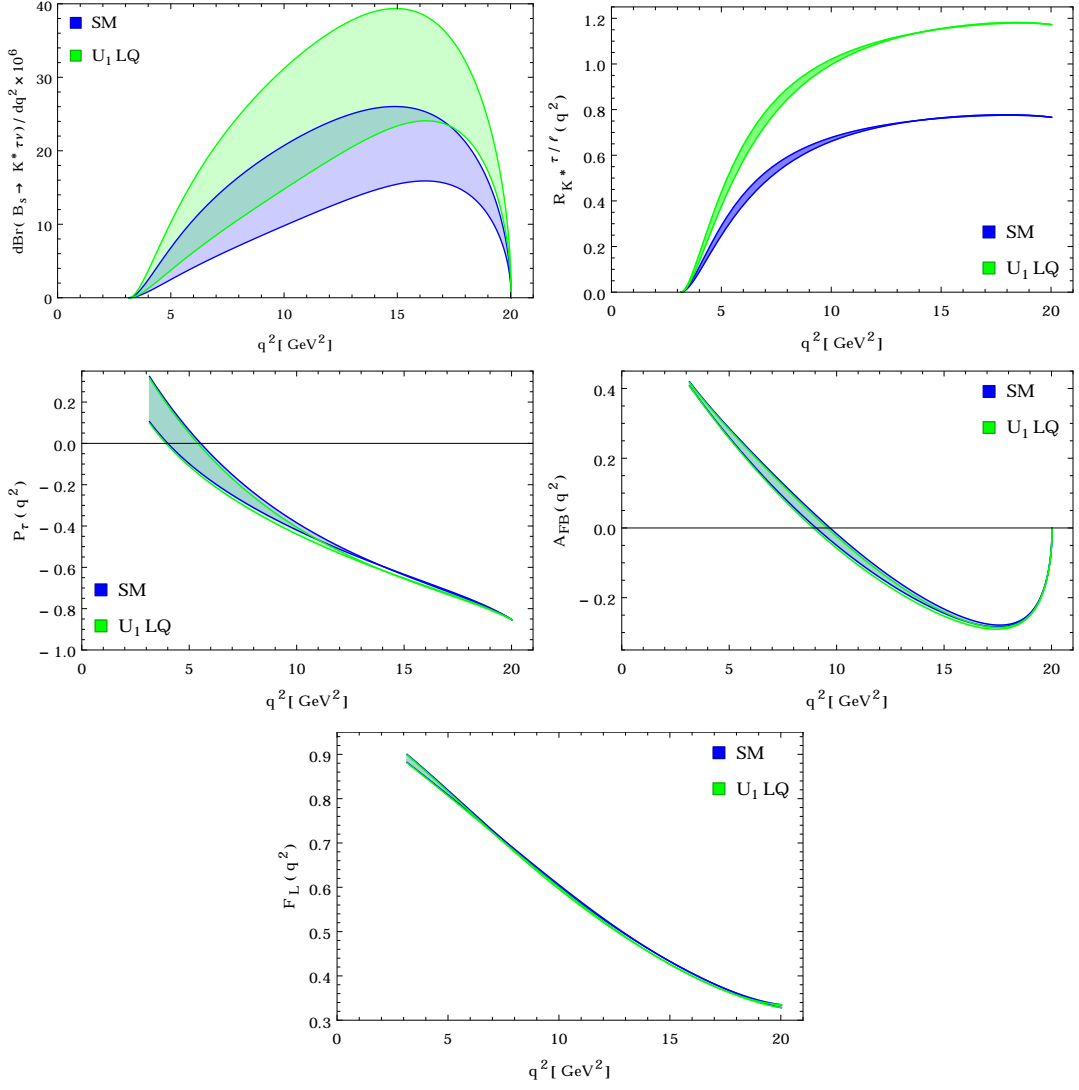


FIG. 6: The q^2 variation plots for the branching fraction, $R_{K^*}^{\tau/\ell}$, P_τ , A_{FB} and F_L of $B_s \rightarrow K^* \tau \bar{\nu}$ decay process.

	$\text{Br}(B_s \rightarrow K^* \tau \bar{\nu})$	$R_{K^*}^{\tau/\ell}$	P_τ	A_{FB}	F_L
SM	$(2.259 \pm 0.449) \times 10^{-4}$	0.580 ± 0.023	-0.534 ± 0.043	-0.135 ± 0.040	0.505 ± 0.039
U_1 LQ	$(3.416 \pm 0.680) \times 10^{-4}$	0.877 ± 0.033	-0.552 ± 0.040	-0.142 ± 0.040	0.500 ± 0.039

TABLE V: Predictions for the observables in $B \rightarrow K^* \tau \bar{\nu}$ decay process in the SM as well as in the LQ model.

VI. CONCLUSIONS

Probing the extension of the SM at the TeV scale is one of the prime goals of LHC experiment. However, in the absence of any direct observation of NP signal at LHC, we need to adopt alternative strategies. In this context, the results LHCb and B factory experiments may be examined seriously to look for any smoking-gun signal of NP beyond the SM. In fact, the recent observation of various flavour anomalies associated with $b \rightarrow c\ell\bar{\nu}$ and $b \rightarrow s\ell^+\ell^-$ transitions may be considered as one of the most imperative hints of NP at the TeV scale. However, it is really a challenging task to explain these appealing set of anomalies in a coherent manner using a single platform, as the NP scales involved in the CC and NC sectors differ significantly. There are only a handful of models which can provide simultaneous solutions to the discrepancies of both these sectors. The vector LQ model, where the SM is extended by an additional TeV scale LQ $U_1(3, 1, 2/3)$ is known to be one such model. Therefore, in this work we have performed a detailed study of the impact of the U_1 LQ on the rare semileptonic decay channels mediated by $b \rightarrow u\tau\bar{\nu}$ transitions. To constrain the new physics parameters we have performed a global fit using various observables in the $b \rightarrow c\ell\bar{\nu}$, $b \rightarrow s\ell^+\ell^-$ as well as the $b \rightarrow u\tau\bar{\nu}$ transitions which show few sigma deviations. After ensuring that we are dealing with scenarios allowed by $b \rightarrow c\ell\bar{\nu}$ as well as $b \rightarrow s\ell^+\ell^-$ anomalies, we made the predictions for different observables of $B \rightarrow (\pi, \rho, \omega)\tau\bar{\nu}$ as well as $B_s \rightarrow (K, K^*)\tau\bar{\nu}$ processes. The list of these observables include branching fractions, lepton non-universality parameters, forward backward asymmetries, lepton polarization asymmetries as well as longitudinal polarization of the final vector mesons. We found that in all these processes the branching fractions as well as the lepton non-universality parameters $R_{P,V}^{\tau/\ell}$ show significant deviation from their corresponding SM predictions whereas the impact of U_1 LQ on other observables is rather mild. Since, the observables $R_{P,V}^{\tau/\ell}$ are fairly clean, i.e., essentially free from hadronic uncertainties, with large deviations from their SM values, it is strongly urged to search for them in the LHCb or Belle II experiments. If such observables are measured, they would provide an indirect signal for the possible existence of TeV scale vector LQ.

Acknowledgments

We thank the organizers of WHEPP 2019 at IIT Guwahati, where this work was initiated. RM acknowledges the support from SERB, Government of India, through grant No. EMR/2017/001448.

-
- [1] J. P. Lees *et al.* [BaBar Collaboration], Phys. Rev. Lett. **109**, 101802 (2012) [arXiv:1205.5442 [hep-ex]].
 - [2] J. P. Lees *et al.* [BaBar Collaboration], Phys. Rev. D **88**, no. 7, 072012 (2013) [arXiv:1303.0571 [hep-ex]].
 - [3] M. Huschle *et al.* [Belle Collaboration], Phys. Rev. D **92**, no. 7, 072014 (2015) [arXiv:1507.03233 [hep-ex]].
 - [4] Y. Sato *et al.* [Belle Collaboration], Phys. Rev. D **94**, no. 7, 072007 (2016) [arXiv:1607.07923 [hep-ex]].
 - [5] S. Hirose *et al.* [Belle Collaboration], Phys. Rev. Lett. **118**, no. 21, 211801 (2017) [arXiv:1612.00529 [hep-ex]].
 - [6] A. Abdesselam *et al.* [Belle Collaboration], arXiv:1904.08794 [hep-ex].
 - [7] R. Aaij *et al.* [LHCb Collaboration], Phys. Rev. Lett. **115**, no. 11, 111803 (2015) [arXiv:1506.08614 [hep-ex]].
 - [8] R. Aaij *et al.* [LHCb], Phys. Rev. Lett. **120** (2018) no.17, 171802 [arXiv:1708.08856 [hep-ex]].
 - [9] R. Aaij *et al.* [LHCb Collaboration], Phys. Rev. D **97** (2018) no.7, 072013 [arXiv:1711.02505 [hep-ex]].
 - [10] R. Aaij *et al.* [LHCb], JHEP **07** (2013), 084 [arXiv:1305.2168 [hep-ex]].
 - [11] R. Aaij *et al.* [LHCb], Phys. Rev. Lett. **111** (2013), 191801 [arXiv:1308.1707 [hep-ex]].
 - [12] R. Aaij *et al.* [LHCb], JHEP **06** (2014), 133 [arXiv:1403.8044 [hep-ex]].
 - [13] R. Aaij *et al.* [LHCb], JHEP **09** (2015), 179 [arXiv:1506.08777 [hep-ex]].
 - [14] R. Aaij *et al.* [LHCb], JHEP **02** (2016), 104 [arXiv:1512.04442 [hep-ex]].
 - [15] R. Aaij *et al.* [LHCb], Phys. Rev. Lett. **125** (2020) no.1, 011802 [arXiv:2003.04831 [hep-ex]].
 - [16] R. Aaij *et al.* [LHCb], Phys. Rev. Lett. **113** (2014), 151601 [arXiv:1406.6482 [hep-ex]].
 - [17] R. Aaij *et al.* [LHCb], JHEP **08** (2017), 055 [arXiv:1705.05802 [hep-ex]].

- [18] R. Aaij *et al.* [LHCb], Phys. Rev. Lett. **122** (2019) no.19, 191801 [arXiv:1903.09252 [hep-ex]].
- [19] A. Abdesselam *et al.* [Belle], [arXiv:1908.01848 [hep-ex]].
- [20] A. Abdesselam *et al.* [Belle], [arXiv:1904.02440 [hep-ex]].
- [21] Y. S. Amhis *et al.* [HFLAV], [arXiv:1909.12524 [hep-ex]].
- [22] R. Aaij *et al.* [LHCb], Phys. Rev. Lett. **120** (2018) no.12, 121801 [arXiv:1711.05623 [hep-ex]].
- [23] R. Dutta and A. Bhol, Phys. Rev. D **96** (2017) no.7, 076001 [arXiv:1701.08598 [hep-ph]].
- [24] A. Abdesselam *et al.* [Belle], [arXiv:1903.03102 [hep-ex]].
- [25] A. K. Alok, D. Kumar, S. Kumbhakar and S. U. Sankar, Phys. Rev. D **95** (2017) no.11, 115038 [arXiv:1606.03164 [hep-ph]].
- [26] S. Bhattacharya, S. Nandi and S. Kumar Patra, Eur. Phys. J. C **79** (2019) no.3, 268 [arXiv:1805.08222 [hep-ph]].
- [27] Q. Y. Hu, X. Q. Li and Y. D. Yang, Eur. Phys. J. C **79** (2019) no.3, 264 [arXiv:1810.04939 [hep-ph]].
- [28] A. K. Alok, D. Kumar, S. Kumbhakar and S. Uma Sankar, Nucl. Phys. B **953** (2020), 114957 [arXiv:1903.10486 [hep-ph]].
- [29] P. Asadi and D. Shih, Phys. Rev. D **100** (2019) no.11, 115013 [arXiv:1905.03311 [hep-ph]].
- [30] C. Murgui, A. Peuelas, M. Jung and A. Pich, JHEP **09** (2019), 103 [arXiv:1904.09311 [hep-ph]].
- [31] M. Blanke, A. Crivellin, T. Kitahara, M. Moscati, U. Nierste and I. Niandi, Phys. Rev. D **100** (2019) no.3, 035035 [arXiv:1905.08253 [hep-ph]].
- [32] R. X. Shi, L. S. Geng, B. Grinstein, S. Jger and J. Martin Camalich, JHEP **12** (2019), 065 [arXiv:1905.08498 [hep-ph]].
- [33] D. Beirevi, M. Fedele, I. Niandi and A. Tayduganov, [arXiv:1907.02257 [hep-ph]].
- [34] S. Sahoo and R. Mohanta, [arXiv:1910.09269 [hep-ph]].
- [35] K. Cheung, Z. R. Huang, H. D. Li, C. D. Lu, Y. N. Mao and R. Y. Tang, [arXiv:2002.07272 [hep-ph]].
- [36] S. Kumbhakar, [arXiv:2007.08132 [hep-ph]].
- [37] A. K. Alok, A. Dighe, S. Gangal and D. Kumar, JHEP **06** (2019), 089 [arXiv:1903.09617 [hep-ph]].
- [38] M. Alguer, B. Capdevila, A. Crivellin, S. Descotes-Genon, P. Masjuan, J. Matias, M. Novoa Brunet and J. Virto, Eur. Phys. J. C **79** (2019) no.8, 714 [arXiv:1903.09578 [hep-ph]].

- [39] J. Aebischer, W. Altmannshofer, D. Guadagnoli, M. Reboud, P. Stangl and D. M. Straub, Eur. Phys. J. C **80** (2020) no.3, 252 [arXiv:1903.10434 [hep-ph]].
- [40] M. Ciuchini, A. M. Coutinho, M. Fedele, E. Franco, A. Paul, L. Silvestrini and M. Valli, Eur. Phys. J. C **79** (2019) no.8, 719 [arXiv:1903.09632 [hep-ph]].
- [41] K. Kowalska, D. Kumar and E. M. Sessolo, Eur. Phys. J. C **79** (2019) no.10, 840 [arXiv:1903.10932 [hep-ph]].
- [42] A. Arbey, T. Hurth, F. Mahmoudi, D. M. Santos and S. Neshatpour, Phys. Rev. D **100** (2019) no.1, 015045 [arXiv:1904.08399 [hep-ph]].
- [43] M. Bauer and M. Neubert, Phys. Rev. Lett. **116** (2016) no.14, 141802 [arXiv:1511.01900 [hep-ph]].
- [44] D. Beirevi, S. Fajfer, N. Konik and O. Sumensari, Phys. Rev. D **94** (2016) no.11, 115021 [arXiv:1608.08501 [hep-ph]].
- [45] S. Fajfer and N. Konik, Phys. Lett. B **755** (2016), 270-274 [arXiv:1511.06024 [hep-ph]].
- [46] S. Sahoo, R. Mohanta and A. K. Giri, Phys. Rev. D **95** (2017) no.3, 035027 [arXiv:1609.04367 [hep-ph]].
- [47] C. H. Chen, T. Nomura and H. Okada, Phys. Lett. B **774** (2017), 456-464 [arXiv:1703.03251 [hep-ph]].
- [48] A. Crivellin, C. Greub, D. Mller and F. Saturnino, Phys. Rev. Lett. **122** (2019) no.1, 011805 [arXiv:1807.02068 [hep-ph]].
- [49] J. Kumar, D. London and R. Watanabe, Phys. Rev. D **99** (2019) no.1, 015007 [arXiv:1806.07403 [hep-ph]].
- [50] C. Cornella, J. Fuentes-Martin and G. Isidori, JHEP **07** (2019), 168 [arXiv:1903.11517 [hep-ph]].
- [51] H. Georgi and S. L. Glashow, Phys. Rev. Lett. **32** (1974), 438-441
- [52] H. Georgi, AIP Conf. Proc. **23** (1975), 575-582
- [53] H. Fritzsch and P. Minkowski, Annals Phys. **93** (1975), 193-266
- [54] P. Langacker, Phys. Rept. **72** (1981), 185
- [55] J. C. Pati and A. Salam, Phys. Rev. D **10** (1974), 275-289
- [56] J. C. Pati and A. Salam, Phys. Rev. D **8** (1973), 1240-1251
- [57] J. C. Pati and A. Salam, Phys. Rev. Lett. **31** (1973), 661-664
- [58] O. U. Shanker, Nucl. Phys. B **206** (1982), 253-272

- [59] B. Schrempp and F. Schrempp, Phys. Lett. B **153** (1985), 101-107
- [60] D. B. Kaplan, Nucl. Phys. B **365** (1991), 259-278
- [61] B. Gripaios, JHEP **02** (2010), 045 [arXiv:0910.1789 [hep-ph]].
- [62] N. Rajeev and R. Dutta, Phys. Rev. D **98** (2018) no.5, 055024 [arXiv:1808.03790 [hep-ph]].
- [63] P. Colangelo, F. De Fazio and F. Loparco, Phys. Rev. D **100** (2019) no.7, 075037 [arXiv:1906.07068 [hep-ph]].
- [64] S. Sahoo and A. Bhol, [arXiv:2005.12630 [hep-ph]].
- [65] P. Colangelo, F. De Fazio and F. Loparco, [arXiv:2006.13759 [hep-ph]].
- [66] M. Tanabashi *et al.* [Particle Data Group], Phys. Rev. D **98** (2018) no.3, 030001
- [67] F. James and M. Roos, Comput. Phys. Commun. **10** (1975), 343-367
- [68] F. James, CERN-D-506.
- [69] R. Alonso, B. Grinstein and J. Martin Camalich, Phys. Rev. Lett. **118** (2017) no.8, 081802 [arXiv:1611.06676 [hep-ph]].
- [70] P. Hamer *et al.* [Belle], Phys. Rev. D **93** (2016) no.3, 032007 [arXiv:1509.06521 [hep-ex]].
- [71] D. M. Straub, [arXiv:1810.08132 [hep-ph]].
- [72] Y. Sakaki, M. Tanaka, A. Tayduganov and R. Watanabe, Phys. Rev. D **88** (2013) no.9, 094012 [arXiv:1309.0301 [hep-ph]].
- [73] J. A. Bailey *et al.* [Fermilab Lattice and MILC], Phys. Rev. D **92** (2015) no.1, 014024 [arXiv:1503.07839 [hep-lat]].
- [74] A. Bharucha, D. M. Straub and R. Zwicky, JHEP **08** (2016), 098 [arXiv:1503.05534 [hep-ph]].
- [75] A. Bazavov *et al.* [Fermilab Lattice and MILC], Phys. Rev. D **100** (2019) no.3, 034501 [arXiv:1901.02561 [hep-lat]].
- [76] R. R. Horgan, Z. Liu, S. Meinel and M. Wingate, Phys. Rev. D **89** (2014) no.9, 094501 [arXiv:1310.3722 [hep-lat]].